Experimental Observation of a Superfluid Gyroscope in a Dilute Bose-Einstein Condensate

E. Hodby, S. A. Hopkins, G. Hechenblaikner, N. L. Smith, and C. J. Foot
Clarendon Laboratory, Department of Physics, University of Oxford, Parks Road, Oxford, OX1 3PU, United Kingdom
(Received 27 September 2002; published 27 August 2003)

We have observed a three-dimensional gyroscopic effect associated with a vortex in a dilute Bose-Einstein condensed gas. A condensate with a vortex possesses a single quantum of circulation, and this causes the plane of oscillation of the scissors mode to precess around the vortex line. We have measured the precession rate of the scissors oscillation. From this we deduced the angular momentum associated with the vortex line and found a value close to $\hbar$ per particle, as predicted for a superfluid.

DOI: 10.1103/PhysRevLett.91.090403 PACS numbers: 03.75.Kk, 05.30.Jp, 67.40.Db, 67.90.+z

The superfluid nature of a dilute gas Bose condensate, most strikingly demonstrated by its response to rotation, is currently an area of great experimental interest. The unique response of a superfluid to an applied torque arises because the presence of its single macroscopic wave function constrains the flow patterns allowed within its bulk. In [1], and later in [2,3], vortices with quantized circulation were observed when the trapping potential confining the atoms was rotated above a critical speed. Such vortices correspond to phase singularities within the gas where the density goes to zero. The quantization of circulation (and hence angular momentum) associated with each vortex demonstrates the presence of a single-valued superfluid wave function within the condensate. Below the critical rotation rate for vortex nucleation, the observation of the oscillation frequency of the scissors mode [4] gave further evidence for the presence of a superfluid wave function by showing that only an irrotational flow pattern (and not a rotational one) was possible in a vortex-free condensate.

In this Letter, we describe the realization of a "superfluid gyroscope" as discussed by Stringari in [4], in an experiment that combines two striking superfluid effects, namely, the production of quantized vortices and the reduced moment of inertia associated with the excitation of the scissors mode. The experiment is performed on a Rb^{87} condensate produced by forced rf evaporative cooling in a time-orbiting potential (TOP) trap [5]. Thus the condensate is held in a harmonic potential with trap frequencies $\omega_x = \omega_y = \omega_\perp$ and $\omega_z \sim 2.8\omega_\perp$, and its shape is oblate spheroidal, i.e., larger in the radial xy plane than along the z axis. The scissors mode is a small-angle oscillation of the condensate relative to the trap potential that is excited by a sudden tilt of the trap, as described in detail elsewhere [6,7]. In the gyroscope experiment we excite the scissors mode oscillation in the xz or yz plane of an axially symmetric condensate containing a vortex along the z axis. In the presence of the vortex the plane of oscillation of the scissors mode precesses slowly around the z axis. In polar coordinates, the scissors oscillation is in the θ direction and the precession is in the ϕ direction as shown in Fig. 1. From the precession rate we deduce the angular momentum associated with the vortex line $\langle L_z\rangle$ and hence show that this angular momentum is quantized in units of $\hbar$ per particle, as predicted for a superfluid.

The relationship between the precession rate Ω and $\langle L_z\rangle$ may be derived by considering the scissors mode as an equal superposition of two counterrotating $m = \pm 1$ modes [8]. These modes represent a condensate whose normal axis is tilted by a small-angle θ from the z axis, and where the plane of this tilt (defined by the normal axis and the z axis) rotates around the z axis at the frequency of the scissors oscillation, $\omega_\pm = \pm\omega_{sc}$, where $\omega_{sc} = (\omega_x^2 + \omega_z^2)^{1/2}$. The symmetry and hence degeneracy of these modes is broken by the presence of axial angular momentum $\langle L_z\rangle$. Provided that the splitting is small compared to ω_{sc}, Ref. [4] predicts a precession frequency Ω given by

$$\Omega = \frac{\omega_+ - \omega_-}{2} = \frac{\langle L_z\rangle}{2mN\langle x^2 + z^2\rangle}, \tag{1}$$

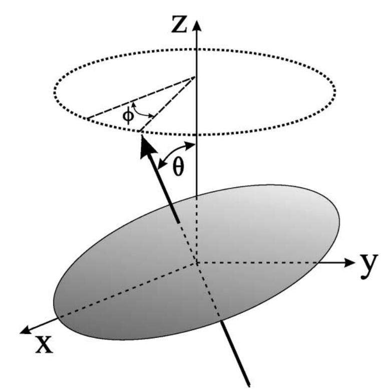

FIG. 1. The gyroscope motion. In equilibrium, the oblate spheroidal condensate (projected outline shown as the grey ellipse) would lie stationary with its normal axis (heavy black arrow) parallel to the z axis. The scissors oscillation involves a fast harmonic oscillation, at ω_{sc}, of the small angle θ between the condensate normal axis and the z axis. When a vortex is present, the plane of this oscillation (initially the xz plane when $\phi = 0$), and then slowly precesses through angle ϕ about the z axis.

 0031-9007/03/91(9)/090403(4)$20.00 090403-1

where N is the total number of atoms in the condensate, m is the atomic mass, and $\langle x^2 + z^2 \rangle$ is the mean value of $x^2 + z^2$ over the condensate. Substituting for $\langle x^2 + z^2 \rangle$ in the case of a harmonically trapped condensate, one obtains [4,9]

$$\Omega = \frac{7\omega_{\rm sc}}{2}\frac{\langle L_z \rangle}{N\hbar}\frac{\lambda^{5/3}}{(1+\lambda^2)^{3/2}}\left(15N\frac{a}{a_{\rm ho}}\right)^{-2/5}, \qquad (2)$$

where $\lambda = \omega_z/\omega_\perp$, $a_{\rm ho} = [\hbar/m(\omega_x\omega_y\omega_z)^{1/3}]^{1/2}$ is the trap harmonic oscillator length, and a is the s-wave scattering length.

Other superfluid gyroscopic effects have been observed, but the three-dimensional interaction between the velocity field of the vortex and the scissors mode of the condensate make this experiment unique. Superfluid gyroscopes of liquid helium exhibit persistent currents in toroidal geometries, with many quanta of circulation [10]. In contrast, we show here that a single vortex of angular momentum $\langle L_z \rangle = N\hbar$ significantly modifies the bulk motion of a trapped Bose-Einstein condensed (BEC) gas in an excited state. This is possible because the vortex produces relative shifts in the excitation spectrum of order ξ/R_0, and in such a dilute system the vortex core size ξ cannot be ignored with respect to the average size of the condensate R_0 [9]. Related experiments with vortex lines in dilute trapped gases are described in [11,12]. The angular momentum of a vortex line was measured in [11] using the precession of a radial breathing mode (a superposition of $m = \pm 2$ quadrupole modes) in the plane perpendicular to the vortex line. In that work, involving the $(x \pm iy)^2$ quadrupole modes, motion is confined to two dimensions and the quadrupole oscillation of the condensate does not affect the vortex line. In contrast, our work is the first observation and measurement of the precession of the $(x \pm iy)z$ quadrupole mode, where the precession occurs in a plane (xy) orthogonal to the collective oscillation (xz or yz). Thus our system undergoes a fully three-dimensional motion, reminiscent of the precession and nutation of a classical spinning top. A detailed study of the gyroscopic motion of this system of a trapped Bose gas containing a vortex has been recently carried out by Nilsen *et al.* [13]; they compare the solution of the hydrodynamic equations with a numerical simulation of the behavior for our experimental conditions using the Gross-Pitaevski equation. Nilsen *et al.* also explore the exact relationship with the classical gyroscope. The motion of the vortex line relative to the condensate is also of interest [13–15]. It has been suggested in [4] that the vortex line might follow oscillatory and precessional motion of the condensate axis, and we present evidence consistent with that view. In [12], unlike the present case, the precession of a vortex line is observed in the absence of any bulk condensate motion, when it is tilted or displaced from the condensate symmetry axes.

The first stage of exciting the superfluid gyroscope is to nucleate a single vortex at the center of a condensate. A detailed discussion of the conditions for vortex nucleation in our apparatus is given in [3]. In summary, the excitation procedure used for this experiment was as follows: First we produced a condensate in an axially symmetric TOP trap with $\omega_\perp/2\pi = 62$ Hz and $\omega_z/2\pi = 175$ Hz. To spin up the condensate we made the trap eccentric ($\omega_x/\omega_y = 1.04$) in a ramp of 0.2 s, with a trap rotation rate of 44 Hz. After holding the condensate in the spinning trap for a further 1 s we ceased the rotation of the trap potential by ramping both the trap rotation rate and the trap eccentricity to zero over 0.4 s. During the whole vortex excitation process, the rf field used for evaporative cooling was maintained at a constant frequency and power; this ensured the rapid removal from the trap of energetic thermal atoms which are an undesirable by-product of the spinning up procedure. This rf shield maintained the temperature at approximately $0.5T_c$.

Equation (2) shows that the precession rate is affected by the number of atoms in the condensate and the angular momentum associated with a vortex line. Our shot-to-shot number variation of $N = 19\,000 \pm 4000$ produces a 10% variation in the precession rate. More significant is the number and position of vortex lines within the condensate, since the precession depends linearly on $\langle L_z \rangle$. In a condensate of finite size, each vortex line is associated with $\hbar$ of angular momentum per particle only if it is exactly centered. The angular momentum associated with an off-center vortex in an axially symmetric, harmonically trapped Thomas-Fermi condensate is [16,17]

$$\langle L_z \rangle = N\hbar\left(1 - \frac{d^2}{R_\perp^2}\right)^{5/2}, \qquad (3)$$

where d is the radial position of the vortex and $R_\perp$ is the radial condensate size. Using our second imaging system that looks along the axis of rotation (z axis), we were able to check that ~90% of the runs started with a single, clearly visible vortex positioned within a third of the condensate radius from the center.

Immediately after making a vortex, the TOP trap was suddenly tilted to excite either the xz- or yz-scissors mode. A detailed description of the tilting procedure is given in [6], but in summary, we apply an additional magnetic field to the TOP trap in the z direction, oscillating in phase with one of the radial TOP bias-field components, B_x or B_y, to excite either the xz- or yz-scissors mode, respectively. The amplitude of this field was 0.55 G, which combined with a 2 G radial bias field tilts the trap by 4.4° and hence excites a scissors oscillation of the same amplitude about the new tilted equilibrium position.

After allowing the oscillation to evolve for a variable time in the trap, we release it and destructively image along the y direction after 12 ms of expansion. By fitting a tilted parabolic density distribution to the image, we can extract the angle of the cloud and thus gradually build up a plot of the scissors oscillation as a function of time. The visibility of the fast scissors oscillation depends on the angle of the cloud projected on the xz plane (the plane perpendicular to the imaging direction) and hence varies at the slow precession frequency Ω. If the oscillation is in the xz plane then the projected amplitude on the image plane is maximum and if it is in the yz plane then the projected amplitude is zero (see Fig. 1). By plotting the scissors oscillation as a function of evolution time, we observe the slowly oscillating visibility and hence extract the precession rate.

Figure 2 shows this plot when the scissors mode was originally excited in the xz plane, perpendicular to the imaging direction. In (a) the condensate contained a vortex, while (b) is a control run using condensates that did not contain a vortex. Each data point was taken 5 times, and the mean and standard deviation are plotted. This averaging was necessary because the slight shot-to-shot variation in the starting conditions leads to slightly different precession rates. The fitting function used was

$$\theta = \theta_{\mathrm{eq}} + \theta_0 \,|\cos\Omega t|\,(\cos\omega_{\mathrm{sc}} t)\, e^{-\gamma t}, \tag{4}$$

with Ω set to zero for Fig. 2(b). In both cases the fast scissors oscillation is clearly visible and the fitted values of $\omega_{\mathrm{sc}}/2\pi$ of (a) 179 Hz and (b) 186 Hz agree reasonably well with the theoretical value of 177 Hz. In the presence of a vortex the visibility shrinks rapidly to zero over 30 ms as the oscillation precesses through 90° to a plane containing the imaging direction. The oscillation visibility grows again after a further 90° precession. In the limit of small tilt angles the variation in oscillation visibility is represented by the $|\cos\Omega t|$ term in Eq. (4). Note that $2\pi/\Omega$ is the time for a full 2π rotation, and hence we expect the visibility to fall from maximum to zero in a quarter period, $\pi/2\Omega$. A fitted value of $\Omega/2\pi = 8.3 \pm 0.7$ Hz is obtained from Fig. 2(a).

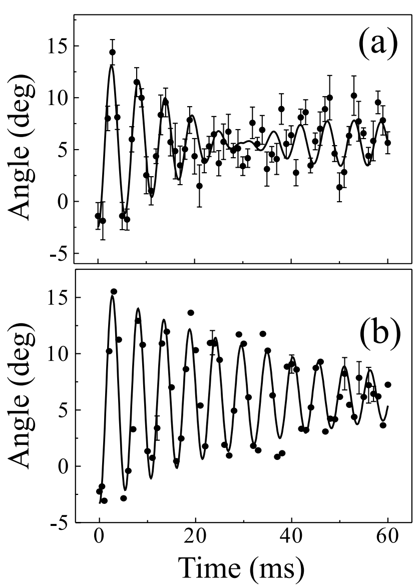

FIG. 2. The angle of the cloud projected on the xz plane when the scissors mode is initially excited in the xz plane, in (a) with a vortex and in (b) without a vortex. In (a) each data point is the mean of 5 runs, with the standard error on each point shown. The solid line is the fitted function given in Eq. (4). In (b) most data points are an average of 2 runs, occasionally 5 runs were taken, and the standard error is shown for these points for comparison with (a).

The revived amplitude is smaller than the initial amplitude due to Landau damping, which occurs at a rate of $\gamma = 23 \pm 7\ \mathrm{s}^{-1}$ from the exponential decay term in Eq. (4). Damping also occurs at a similar rate of $\gamma = 25 \pm 5\ \mathrm{s}^{-1}$ in the control run, Fig. 2(b), without the presence of a vortex. Note that in (b) the condensate underwent the same spinning up procedure but at a trap rotation rate of 35 Hz, just too slow to create vortices. This ensured that in both cases the condensates were at the same temperature and hence had comparable Landau damping rates. The damping rates of approximately $24\ \mathrm{s}^{-1}$ at a temperature of $0.5T_c$ agree well with the data about the temperature dependence of the scissors mode published in [18]. The control plot also confirmed that an axially symmetric condensate must have $L_z = 0$ unless a vortex line is present and hence the vortex is essential for precession.

Figure 3 shows the same experiment but with the scissors mode initially excited along the imaging direction so that the initial visibility is zero. The appropriate fitting function in this case is

$$\theta = \theta_{\mathrm{eq}} + \theta_0 \,|\sin\Omega t|\,(\cos\omega_{\mathrm{sc}} t)\, e^{-\gamma t}. \tag{5}$$

There was insufficient data to fit the Landau damping rate accurately in this case, and so the value of γ was fixed at

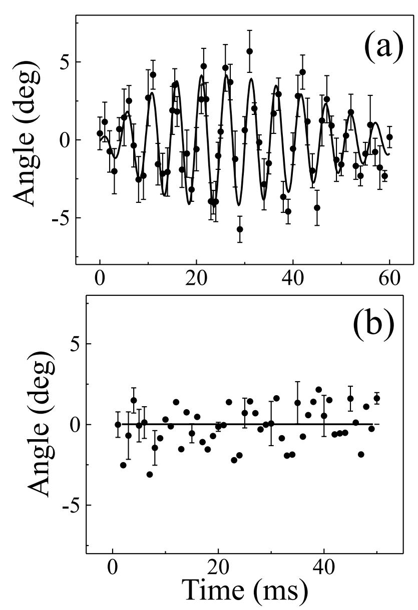

FIG. 3. As for Fig. 2 but with the scissors mode initially excited in the yz plane and Eq. (5) as the fitting function (solid line).

24.2 s^{-1}, as determined from the data of Fig. 2. In the presence of a vortex [Fig. 3(a)] the visibility of the scissors oscillation grows as the oscillation plane rotates through 90° to the xz plane. This growth of an oscillation is perhaps a more significant proof of precession than the initial decrease of amplitude in Fig. 2(a), since it cannot be explained by any damping effect. Figure 3(b) shows the data obtained when there was no vortex so the oscillation remained in the yz plane, with zero angle projected onto the xz direction. Note that the mean angles in Fig. 2(a) and 3(a) are different. In Fig. 2 the trap tilt occurs in the xz plane, and so the mean angle θ_{eq} is the tilt angle of the trapping potential (the angle of cloud angle at equilibrium). Whereas in Fig. 3 the tilt is in the yz plane, the mean angle in the imaging plane is zero.

The precession rate deduced from Fig. 3(a) is $\Omega/2\pi = 7.2 \pm 0.6$ Hz, which agrees within the stated errors with the precession rate obtained from Fig. 2(a). Combining the results for the gyroscope experiments initiated by tilting in the xz and yz planes gives an average precession frequency of $\Omega_{exp}/2\pi = 7.7 \pm 0.5$ Hz. This result is in reasonable agreement with the detailed calculations in Ref. [13] which predict a precession frequency of 6.5 Hz by numerical solution of the Gross-Pitaevskii equation for the conditions of our experiment. To calculate the angular momentum per particle associated with a vortex line we use Eq. (2) which is applicable in the hydrodynamic regime and find an angular momentum per particle of $\langle l_z \rangle = (1.07 \pm 0.13)\hbar$. The uncertainty in this quantity is mainly due to the uncertainty in the number of atoms ($N = 19\,000 \pm 4000$). This result is in excellent agreement with the value of $\hbar$ per particle predicted by quantum mechanics.

Finally, we discuss the motion of the vortex core, prompted by the suggestion in [4] that it might exactly follow the axis of the condensate. Images taken perpendicular to the vortex core are necessary to show the angle of the core relative to the axis of the condensate. However, in a dense condensate the vortex core is too small to have a discernible effect on the integrated absorption profile. Thus we reduced the number of atoms in the condensate to $\leq 10\,000$ to obtain many such images, and three examples are shown in Fig. 4. Vortices were clearly visible on 50% of the experimental runs, and within the limits of the imaging system resolution and pixel to pixel noise, the vortex lines in these shots tend to be aligned with the condensate axis. Also, slight bending of the vortex lines cannot be ruled out. However, owing to the small number of atoms, we were unable to conclusively fit any function for the angle (or indeed straightness) of the vortex core relative to the condensate axis.

In conclusion, we have observed a superfluid gyroscope effect in a trapped Bose-Einstein condensate, in which a single quantum of circulation (a single vortex line) affects the bulk scissors motion of the condensate and causes it to precess. By observing the precession rate we are able to measure the angular momentum associated with the vortex line. Our result of $(1.07 \pm 0.13)N\hbar$ agrees well with $N\hbar$, the quantum of angular momentum that is predicted to be associated with each centered vortex line. The gyroscope provides a further tool to explore the intriguing features of rotating Bose-Einstein condensed gases such as the stability and lifetime of vortices and the further study of the decay mechanisms of quadrupole oscillations into kelvons [14].

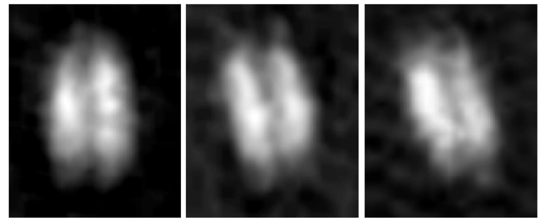

FIG. 4. Three examples of absorption images, taken along the y direction and perpendicular to the core of the vortex after 12 ms of expansion, show the vortex core roughly following the angle of the axis of the condensate during the gyroscope motion. These images were taken with a smaller condensate density ($N \leq 10\,000$), so that the vortex core [of radius $(8\pi na)^{-1/2}$] was large enough to have a significant effect on the integrated absorption profile. White (black) corresponds to a high (low) density of atoms.

We acknowledge support from the EPSRC, St. John's College, Oxford (G. H.), and Christ Church College, Oxford (E. H.). We also thank Graham Quelch for his technical support.

[1] K.W. Madison *et al.*, Phys. Rev. Lett. **84**, 806 (2000).
[2] J. R. Abo-Shaeer *et al.*, Science **292**, 476 (2001).
[3] E. Hodby *et al.*, Phys. Rev. Lett. **88**, 010405 (2002).
[4] S. Stringari, Phys. Rev. Lett. **86**, 4725 (2001).
[5] M. H. Anderson *et al.*, Science **269**, 198 (1995).
[6] O. M. Maragò *et al.*, Phys. Rev. Lett. **84**, 2056 (2000).
[7] D. Guéry-Odelin and S. Stringari, Phys. Rev. Lett. **83**, 4452 (1999).
[8] S. Stringari, Phys. Rev. Lett. **77**, 2360 (1996).
[9] A. A. Svidzinsky and A. L. Fetter, Phys. Rev. A **58**, 3168 (1998).
[10] J. R. Clow and J. D. Reppy, Phys. Rev. A **5**, 424 (1972).
[11] F. Chevy, K.W. Madison, and J. Dalibard, Phys. Rev. Lett. **85**, 2223 (2000).
[12] B. P. Anderson *et al.*, Phys. Rev. Lett. **85**, 2857 (2000); P. C. Haljan *et al.*, Phys. Rev. Lett. **86**, 2922 (2001).
[13] H. M. Nilsen, D. McPeake, and J. F. McCann, J. Phys. B **36**, 1703 (2003).
[14] V. Bretin *et al.*, cond-mat/0211101.
[15] J. E. Williams *et al.*, Phys. Rev. Lett. **88**, 070401 (2002).
[16] M. Guilleumas and R. Graham, Phys. Rev. A **64**, 033607 (2001).
[17] A. Fetter (private communication).
[18] O. Maragò *et al.*, Phys. Rev. Lett. **86**, 3938 (2001).